High-p_T processes measured with ALICE at the LHC

Jacek Otwinowski[*][†]

GSI Helmholtz Centre for Heavy Ion Research, Darmstadt, Germany
E-mail: j.otwinowski@gsi.de

The study of single-particle and jet production in heavy-ion collisions provides insights into the density of the medium and the energy-loss mechanisms. The observed suppression of high-p_T particle production is generally attributed to energy loss of partons as they propagate through the hot and dense QCD medium - Quark-Gluon-Plasma (QGP). Such measurements allow the characterization of the QGP, the deconfined state of quarks and gluons, predicted by QCD. In these proceedings we present the analysis results of Pb–Pb collisions at $\sqrt{s_{NN}} = 2.76$ TeV recorded by ALICE. The nuclear modification factors (R_{AA}) and the results from jet reconstruction in Pb–Pb are presented. Comparison with other measurements and with theory models is discussed.

Xth Quark Confinement and the Hadron Spectrum,
October 8-12, 2012
TUM Campus Garching, Munich, Germany

---

[*]Speaker.

[†]On behalf of the ALICE Collaboration

1. Introduction

This paper reports on measurements of single-particle spectra and jets as a function of transverse momentum (p_T) and event centrality in Pb–Pb collisions at $\sqrt{s_{NN}} = 2.76$ TeV recorded by ALICE [1] in the fall of 2010 and 2011.

Previous results from the Relativistic Heavy Ion Collider (RHIC) [2–11] showed that hadron production at high p_T in central Au–Au collisions at $\sqrt{s_{NN}} = 200$ GeV is suppressed by a factor 4–5 compared to expectations from an independent superposition of nucleon-nucleon collisions. This observation is typically expressed in terms of the nuclear modification factor

$$R_{AA}(p_T) = \frac{\mathrm{d}^2 N_{ch}^{AA}/\mathrm{d}\eta\,\mathrm{d}p_T}{\langle T_{AA}\rangle \mathrm{d}^2 \sigma_{ch}^{pp}/\mathrm{d}\eta\,\mathrm{d}p_T} \tag{1.1}$$

where N_{ch}^{AA} and σ_{ch}^{pp} represent the charged particle yield in nucleus-nucleus (AA) collisions and the cross section in pp collisions, respectively. The nuclear overlap function T_{AA} is calculated from the Glauber model [12] and averaged over each centrality interval, $\langle T_{AA}\rangle = \langle N_{coll}\rangle/\sigma_{inel}^{NN}$, where $\langle N_{coll}\rangle$ is the average number of binary nucleon-nucleon collisions and σ_{inel}^{NN} is the inelastic nucleon-nucleon cross section. In absence of nuclear modifications R_{AA} is equal to unity at high p_T.

2. R_{AA} of charged particles

The nuclear modification factors as a function of p_T for nine centrality intervals [13] are shown in Fig.1. In peripheral collisions (70–80%), only moderate suppression ($R_{AA} = 0.6$–0.7) and a weak p_T dependence are observed. Towards more central collisions, a pronounced minimum at about $p_T = 6$–7 GeV/c develops while for $p_T > 7$ GeV/c there is a significant rise of the nuclear modification factor. This rise becomes gradually less steep with increasing p_T. In the most central collisions (0–5%), the yield is most suppressed, $R_{AA} \approx 0.13$ at $p_T = 6$–7 GeV/c, and R_{AA} reaches ≈ 0.4 with no significant p_T dependence for $p_T > 30$ GeV/c.

The ALICE measurement of R_{AA} in the most central Pb–Pb collisions (0–5%) [13] is compared to the CMS result [14] in Fig. 2 (left). Both measurements agree within their respective statistical and systematic uncertainties. In Fig. 2 (left), the measured R_{AA} for 0–5% central collisions is also compared to model predictions. All selected models use RHIC data to calibrate the medium density. All model calculations, except WHDG [15] , use a hydrodynamical description of the medium, but different extrapolation assumptions from RHIC to LHC. A variety of energy loss formalisms is used. An increase of R_{AA} due to a decrease of the relative energy loss with increasing p_T is seen for all the models. The curves labeled WHDG, ASW, and Higher Twist (HT) are based on analytical radiative energy loss formulations that include interference effects. Of those curves, the multiple soft gluon approximation (ASW [16]) and the opacity expansion (WHDG [15]) show a larger suppression than seen in the measurement, while one of the HT curves (Chen [17]) with lower parton density provides a good description. The other HT (Majumder [18]) curve shows a stronger rise with p_T than measured. The elastic energy loss model by Renk (elastic) [19] does not rise steeply enough with p_T and overshoots the data at low p_T. The YaJEM-D model [20],
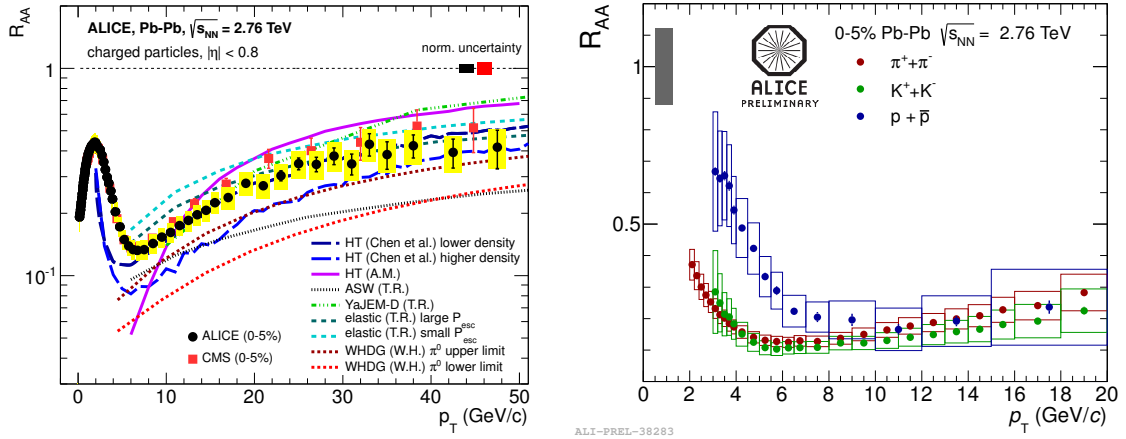
2
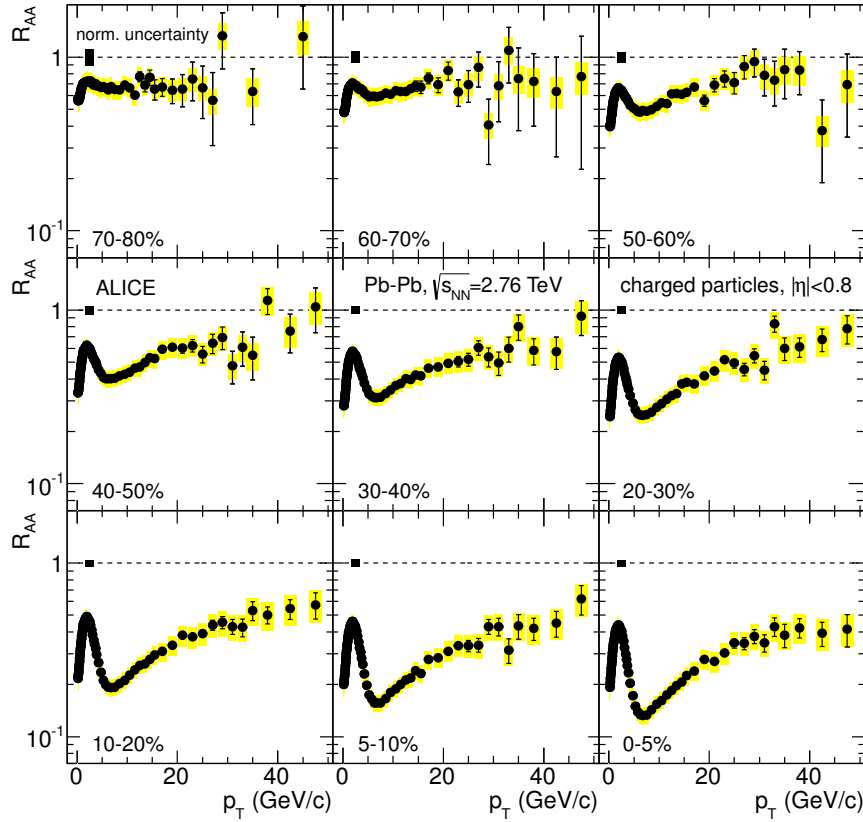
Figure 1: R_{AA} for charged particles as a function of p_T in nine centrality intervals [13]. Normalization uncertainties are shown as the boxes at $R_{AA} = 1$.

which is based on medium-induced virtuality increases in a parton shower, shows too strong a p_T-dependence of R_{AA} due to a formation time cut-off.

A more systematic study of the energy loss formalisms, preferably with the same model(s) for the medium density is needed to rule out or confirm the various effects. Deviations of the nuclear parton distribution functions (PDFs) from a simple scaling of the nucleon PDF with mass number A (e.g. shadowing) are also expected to affect the nuclear modification factor. These effects are predicted [21] to be small for $p_T > 10$ GeV/c at the LHC and will be quantified in future p–Pb measurements.

## 3. R_{AA} of identified hadrons

The measurement of pions, kaons and protons allows us to study the suppression pattern for mesons and baryons, which gives a handle on how to separate quark and gluon energy loss [22]. The analysis of charged pions, kaons and protons at high p_T is based on statistical particle identification using the specific energy loss dE/dx in the TPC [23]. In the region of the relativistic rise of the energy loss ($p_T > 3$ GeV/c), the separation of pions from kaons and protons is nearly indepen-

Figure 2: Left: R_{AA} for charged particles as a function of p_T in central Pb–Pb collisions [13] in comparison to CMS result [14] and model predictions [15–20]. **Right:** R_{AA} for charged pions, kaons and protons as a function of p_T in central Pb–Pb collisions. **Both:** Normalization uncertainties are shown as the boxes at $R_{AA} = 1$.

dent of p_T out to $p_T = 50$ GeV/c. The fraction of pions, kaons and protons from all charged particles is determined in bins of p_T by fitting the dE/dx distribution with four Gaussians for electrons, pions, kaons and protons. The R_{AA} for charged pions, kaons and protons identified in central Pb–Pb collisions are shown in Fig. 2 (right). Production of pions, kaons and protons is strongly suppressed in central Pb–Pb collisions. The yields are most suppressed at $p_T = 6$–8 GeV/c, $R_{AA} \simeq 0.1$–0.2 for all particle species as expected from the R_{AA} of charged particles shown in Fig. 2 (left). For $p_T < 7$ GeV/c, the R_{AA} for pions is similar to that for kaons and is smaller than for protons, which is in line with an enhanced baryon production observed in central Pb–Pb collisions [24]. For $p_T > 7$ GeV/c, the R_{AA} for pions, kaons and protons approach the same value.

The measurement of heavy flavour production at high p_T provides unique observables of jet quenching. The suggestion that massive quarks experience reduced energy loss due to the suppression of forward radiation ("dead cone effect") has not been borne out by measurements at RHIC. The R_{AA} measured for high-p_T D mesons [25], heavy-flavour decay muons (c,b $\rightarrow \mu$) [26] and charged particles [13] as a function of collision centrality measured by ALICE are shown in Fig. 3 (left). For comparison, the R_{AA} for non-prompt J/ψ originating from the B-meson decays measured by CMS [27] is also shown. Heavy flavour production at high p_T ($p_T > 6$ GeV/c) is strongly suppressed in central Pb–Pb collisions, $R_{AA} \simeq 0.2$–0.4. The suppression pattern is similar for heavy flavour measured by ALICE in central and forward rapidities. The data indicate that there might be a hierarchy in the suppression of the light and heavy flavour, $R_{AA}^{B} > R_{AA}^{D} > R_{AA}^{\text{light flavour}}$. The D-meson R_{AA} measured as a function of p_T in the most central Pb–Pb collisions is compared to the R_{AA} for charged particles and pions in Fig. 3 (right). Data show that the R_{AA} of D mesons is consistent with the R_{AA} of light-flavour hadrons at high p_T (> 8 GeV/c). Higher statistics of Pb–Pb data and comparison data in p–Pb collisions should allow us to study this region with more precision and disentangle initial-state nuclear effects, which could be different for light and heavy flavour.
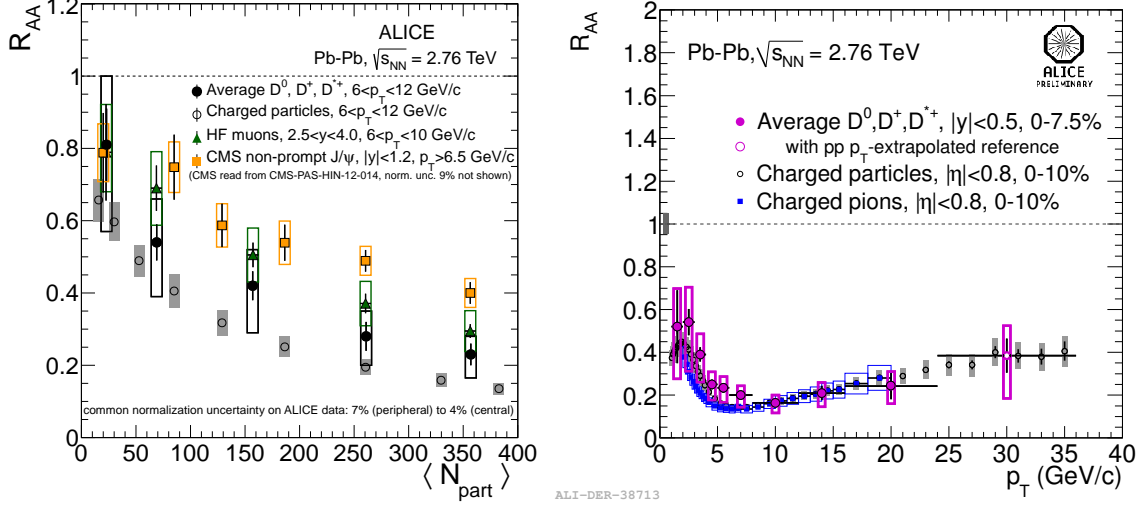
Figure 3: Left: R_{AA} for D mesons [25], heavy-flavour decay muons (c,b$\rightarrow \mu$) [26] and charged particles [13] as a function of collision centrality in comparison to non-prompt J/ψ from CMS [27]. **Right:** R_{AA} for D mesons, charged particles and charged pions as a function of p_T in central Pb–Pb collisions. Common normalization uncertainties on ALICE data are shown as the box at $R_{AA} = 1$.

4. R_{AA} of charged jets

We present results for the jets reconstructed from the charged particles in Pb–Pb collisions measured in 2010. The jet reconstruction with charged and neutral particles (2011 run) is being finalized. The particle tracks are reconstructed using the Time Projection Chamber (TPC) and vertexing information from the Inner Tracking System (ITS). This ensures maximum azimuthal angle (ϕ) uniformity of reconstructed tracks with transverse momenta down to $p_T = 150$ MeV/c.

The jets are reconstructed using the anti-k_T algorithm [28] and are corrected for the background in each event using the jet area A with $p_{T,jet}^{ch} = p_{T,jet}^{rec} - \rho \cdot A$. Here, the background density ρ is calculated on an event-by-event basis as the median for the p_T/A ratio of reconstructed k_T-clusters in $|\eta| < 0.5$ by using k_T algorithm [29]. In addition, the charged jets are corrected for the background fluctuations using an unfolding procedure [30].

The p_T spectra for jets reconstructed in Pb–Pb collisions from charged particles with $p_T > 0.15$ and jet radius R = 0.2 are shown in Fig. 4 (left). The measurement was done for inclusive (unbiased) jets and for jets with the threshold on the leading particle p_T requirement ($p_T > 5$ GeV/c and $p_T > 10$ GeV/c). The p_T spectra for inclusive jets are similar to those for the jets with the leading particle selection indicating that the unfolding procedure deals properly with the background at low p_T (large background fluctuations) and there is rather a weak softening of the fragmentation in central Pb–Pb collisions.

The R_{AA}^{Pythia} for charged jets as a function of p_T in central Pb-Pb collisions in comparison to model calculations (JEWEL [31]) is shown in Fig. 4 (right). The R_{AA}^{Pythia} was constructed using the p_T spectrum for charged jets from Pythia [32] as a pp reference. A strong charged jet suppression is observed with $R_{AA} \simeq 0.2$–0.4 in central Pb–Pb collisions which is consistent with the R_{AA} measured
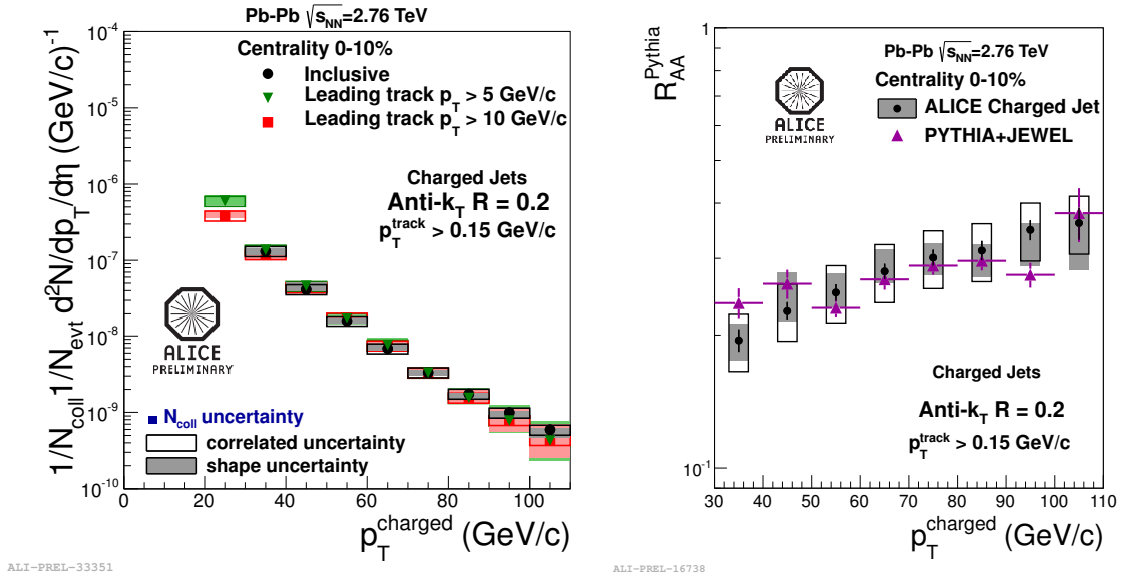
Figure 4: Left: p_T spectra for inclusive charged jets and for jets with the threshold on the leading particle p_T. **Right:** R_{AA} for charged jets in central Pb–Pb collisions in comparison to the model calculations [31]. pp reference spectrum for R_{AA}^{Pythia} based on Pythia [32].

for the charged particles [13], and is in agreement with the ATLAS [33] and CMS [34] results. A good agreement between the JEWEL model calculations and data is observed.

5. Summary

The results indicate a strong suppression of charged particle production in Pb–Pb collisions at $\sqrt{s_{NN}} = 2.76$ TeV and a characteristic centrality and p_T dependence of the nuclear modification factors. The data indicate that there might be a hierarchy in the suppression of the light and heavy flavour at high-p_T (> 6 GeV/c), $R_{AA}^{B} > R_{AA}^{D} > R_{AA}^{light\ flavour}$. The nuclear modification factor for charged jets is similar to that for charged particles, and is in agreement with the ATLAS and CMS results. The comparison of ALICE data to model calculations indicates a large sensitivity of high-p_T particle production to details of energy loss mechanisms.

References

[1] K. Aamodt *et al.* (ALICE Collaboration), JINST **3** (2008) S08002.

[2] I. Arsene *et al.* (BRAHMS Collaboration), Nucl. Phys. **A 757** (2005) 1.

[3] B. B. Back *et al.* (PHOBOS Collaboration), Nucl. Phys. **A 757** (2005) 28.

[4] J. Adams *et al.* (STAR Collaboration), Nucl. Phys. **A 757** (2005) 102.

[5] K. Adcox *et al.* (PHENIX Collaboration), Nucl. Phys. **A 757** (2005) 184.

[6] D. d´Enterria, Phys. Lett. B **596** (2004) 32.

[7] K. Adcox *et al.* (PHENIX Collaboration), Phys. Rev. Lett. **88** (2001) 022301.

[8] C. Adler *et al.* (STAR Collaboration), Phys. Rev. Lett. **89** (2002) 202301.

[9] J. Adams *et al.* (STAR Collaboration), Phys. Rev. Lett. **91** (2003) 172302.

[10] S. S. Adler *et al.* (PHENIX Collaboration), Phys. Rev. C **69** (2004) 034910.

[11] A. Adare *et al.* (PHENIX Collaboration), Phys. Rev. Lett. **101** (2008) 232301.

[12] M. Miller, K. Reygers, S. Sanders and P. Steinberg, Annu. Rev. Nucl. Part. Sci. **57** (2007) 205.

[13] K. Aamodt *et al.* (ALICE Collaboration), arXiv:1208.2711 [hep-ex].

[14] S. Chatrchyan *et al.* (CMS Collaboration), Eur. Phys. J. C **72** (2012) 1945.

[15] W. A. Horowitz and M. Gyulassy, Nucl. Phys. **A 872** (2011) 265.

[16] C. A. Salgado and U. A. Wiedemann, Phys. Rev. D **68** (2003) 014008.

[17] X.-F. Chen, T. Hirano, E. Wang, X.-N. Wang and H. Zang, Phys. Rev. C **84** (2011) 034902.

[18] A. Majumder and B. Muller, Phys. Rev. Lett. **105** (2010) 252002.

[19] T. Renk, H. Holopainen, R. Paatelainen and K. J. Eskola, Phys. Rev. C. **84** (2011) 014906.

[20] T. Renk, Phys. Rev. C **83** (2011) 024908.

[21] W. A. Horowitz and M. Gyulassy, Nucl. Phys. **A 872** (2011) 265.

[22] B. Mohanty *et al.* (STAR Collaboration), J. Phys. G: Nucl. Part. Phys. **35** (2008) 104006.

[23] P. Christiansen *et al.* (ALICE Collaboration), arXiv:1208.5368 [nucl-ex].

[24] A. Ortiz Velasquez *et al.* (ALICE Collaboration), arXiv:1210.6995 [hep-ex].

[25] Abelev *et al.* (ALICE Collaboration), JHEP **9** (2012) 112

[26] Abelev *et al.* (ALICE Collaboration), Phys. Rev. Lett. **109** (2012) 112301

[27] S. Chatrchyan *et al.* (CMS Collaboration), arXiv:1201.5069 [nucl-ex], CMS-PAS-HIN-12-14 (2012).

[28] M. Cacciari and G. P. Salam, Phys. Lett. B **641** (2006) 57.

[29] M. Cacciari and G. P. Salam, Phys. Lett. B **659** (2008) 119.

[30] B. Abelev *et al.* (ALICE Collaboration), JHEP **1203** (2012) 53.

[31] K. C. Zapp, F. Krauss and U. A. Wiedemann, arXiv:1111.6838 [hep-ph].

[32] T. Sjostrand, S. Mrenna, P. Skands, PYTHIA 6.4 Physics and Manual, JHEP **05** (2006) 026, arXiv:hep-ph/0603175.

[33] G. Aad *et al.* (ATLAS Collaboration), arXiv:1208.1967 [hep-ex].

[34] S. Chatrchyan *et al.* (CMS Collaboration), CMS-PAS-HIN-12-004.

PoS(Confinement X)170